

Alterations in Lipid Signaling Underlie Lipodystrophy Secondary to AGPAT2 Mutations

Angela R. Subauste,¹ Arun K. Das,¹ Xiangquan Li,¹ Brandon Elliot,¹ Charles Evans,¹ Mahmoud El Azzouny,² Mary Treutelaar,¹ Elif Oral,¹ Todd Leff,³ and Charles F. Burant^{1,4}

Congenital generalized lipodystrophy (CGL), secondary to AGPAT2 mutation is characterized by the absence of adipocytes and development of severe insulin resistance. In the current study, we investigated the adipogenic defect associated with AGPAT2 mutations. Adipogenesis was studied in muscle-derived multipotent cells (MDMCs) isolated from vastus lateralis biopsies obtained from controls and subjects harboring AGPAT2 mutations and in 3T3-L1 preadipocytes after knockdown or overexpression of AGPAT2. We demonstrate an adipogenic defect using MDMCs from control and CGL human subjects with mutated AGPAT2. This defect was rescued in CGL MDMCs with a retrovirus expressing AGPAT2. Both CGL-derived MDMCs and 3T3-L1 cells with knockdown of AGPAT2 demonstrated an increase in cell death after induction of adipogenesis. Lack of AGPAT2 activity reduces Akt activation, and overexpression of constitutively active Akt can partially restore lipogenesis. AGPAT2 modulated the levels of phosphatidic acid, lysophosphatidic acid, phosphatidylinositol species, as well as the peroxisome proliferator-activated receptor γ (PPAR γ) inhibitor cyclic phosphatidic acid. The PPAR γ agonist pioglitazone partially rescued the adipogenic defect in CGL cells. We conclude that AGPAT2 regulates adipogenesis through the modulation of the lipome, altering normal activation of phosphatidylinositol 3-kinase (PI3K)/Akt and PPAR γ pathways in the early stages of adipogenesis. *Diabetes* 61:2922–2931, 2012

Lipodystrophy and lipotrophy syndromes are characterized by congenital or acquired decreases in adipose tissue, which are associated with severe metabolic consequences (1). Two phenotypes, congenital generalized lipodystrophy (CGL) and familial partial lipodystrophy, are recognized with different degrees of loss of body fat. CGL has been linked with mutations in the *BSL2*, *CAVI*, and *AGPAT2* genes (2–4). AGPAT2 is one of a family of 11 related proteins with acyl transferase activity, with AGPAT2 shown to mediate acylation of lysophosphatidic acid (LPA) to form phosphatidic acid (PA), which serves as a precursor for triacylglycerol and phospholipid synthesis (5). Structure-function studies of AGPAT2 mutations identified in CGL patients demonstrated reduced conversion of LPA to PA after overexpression in CHO cells, suggesting that reduced

AGPAT2 enzymatic activity underlies the CGL clinical phenotype (6).

AGPAT2 expression is upregulated in a number of tumors, and small-molecule inhibitors have been developed that specifically inhibit AGPAT2, but not AGPAT1, activity (7,8). Treatment of tumor cell lines with these agents results in the attenuation of a number of signaling pathways, including both the Ras/Raf/extracellular signal-related kinase (Erk) and phosphatidylinositol 3-kinase (PI3K)/Akt pathways, and results in cell death. Studies have suggested that AGPAT2 may regulate adipogenesis, but, to date, the mechanism by which AGPAT2 may regulate this process has not been defined (10).

Mesenchymal progenitor cells can differentiate along either adipogenic or myogenic pathways. In particular, it has been shown that in vitro mouse satellite cells can directly differentiate into adipocytes (11–13). In this study, we used muscle-derived multipotent cells (MDMCs) from patients with CGL together with 3T3-L1 cells to study the mechanisms by which AGPAT2 supports adipogenesis. We demonstrate that human cells carrying the AGPAT2 mutation have disrupted adipogenesis with cell death. Similar results were obtained in 3T3-L1 cells with AGPAT2 loss of function. The defect in adipogenesis was associated with disruption of PI3K/Akt signaling and peroxisome proliferator-activated receptor γ (PPAR γ) transactivation, likely through the modulation of the lipome early in the differentiation process.

RESEARCH DESIGN AND METHODS

Human muscle biopsies and MDMC isolation. The institutional review boards of the University of Michigan approved the study protocol, and all subjects gave written informed consent. A percutaneous muscle biopsy was obtained from the lateral portion of the vastus lateralis. The biopsy (~100 mg) was minced and digested in collagenase-dispase (10 and 1 mg/mL, respectively) for 30 min. Nondigested tissue was allowed to sediment, and the supernatant was filtered (70 μ m). The supernatant was centrifuged and preplated on type I collagen-coated dishes for 4 h and transferred to collagen-coated dishes (14).

Cell culture and induction of differentiation. MDMCs were maintained in an undifferentiated state in Ham-F10 media/20% FBS/0.5% chicken embryo with antibiotic and antifungals. 3T3-L1 preadipocytes were propagated and maintained in Dulbecco's modified Eagle's medium containing 10% (volume for volume) FBS with antibiotic and antifungals. Differentiation of 3T3-L1 cells was as previously described (15). To induce differentiation of human MDMCs, 2-day postconfluent cells were fed Dulbecco's modified Eagle's medium with insulin (I), dexamethasone (D), and 3-isobutyl-1-methylxanthine (M) and 10% FBS. On day 3, cells were incubated in I media for 2 days and then in IDM for 2 days. This process was repeated for three cycles, until day 21. Oil Red O staining was performed as previously described (15).

3T3-L1 cells were transfected with 20 nmol/L AGPAT1 or AGPAT2 small interfering RNA (siRNA) SMARTpools (Dharmacon, Lafayette, CO) or siCONTROL nontargeting siRNA using Dharmafect 3 transfection reagent. For cells undergoing differentiation, transfection was performed on day -2 of differentiation. Relative AGPAT mRNA levels were determined after 48 h. For overexpression experiments, cells were infected with retrovirus expressing either green fluorescent protein (GFP) or GFP-AGPATs and selected with

From the ¹Department of Internal Medicine, University of Michigan, Ann Arbor, Michigan; the ²Department of Chemistry, University of Michigan, Ann Arbor, Michigan; the ³Department of Pathology, Wayne State University, Detroit, Michigan; and the ⁴Department of Molecular and Integrative Physiology, University of Michigan, Ann Arbor, Michigan.

Corresponding author: Charles F. Burant, burantc@umich.edu.

Received 4 January 2012 and accepted 24 May 2012.

DOI: 10.2337/db12-0004

This article contains Supplementary Data online at <http://diabetes.diabetesjournals.org/lookup/suppl/doi:10.2337/db12-0004/-/DC1>.

© 2012 by the American Diabetes Association. Readers may use this article as long as the work is properly cited, the use is educational and not for profit, and the work is not altered. See <http://creativecommons.org/licenses/by-nc-nd/3.0/> for details.

G418 for 1 week. For transient expression, cells were transfected with V5-tagged AGPAT1, AGPAT2, or empty vector.

Reverse transcriptase PCR analysis. cDNA was synthesized using random hexamers (Promega Biosciences) from 1 μ g of cellular RNA. Expression of the specific genes was assessed by quantitative reverse transcriptase PCR, as previously described (15), using 18s mRNA to normalize expression.

Analysis of cell death by flow cytometry. MDMCs and 3T3-L1 cells were differentiated as previously described, harvested at defined intervals, fixed with 90% ethanol, and incubated with a staining solution containing RNase A (30 μ g/mL) and propidium iodide (50 μ g/mL) in PBS. Cellular DNA content was analyzed by flow cytometry using a Becton Dickinson laser-based flow cytometer. At least 1,000 events were used for each analysis.

Western blot. Cells were lysed in a solubilizing buffer and processed for Western blot analysis as previously described.

Immunostaining and immunofluorescence microscopy. Cells were fixed in 4% formaldehyde in PBS for 15 min at room temperature, permeabilized, and blocked with 0.03% Triton X-100 and 10% normal goat serum for 30 min at room temperature, followed by incubation with specific antibodies in 10% normal goat serum overnight at 4°C and developed with secondary fluorescent-conjugated antibodies.

Phosphoinositide analysis. For phosphatidylinositol 4-phosphate (PIP) analyses, lipids were extracted from cultured cells (100-mm plate) and eluted as previously described (16,17).

Reverse-phase liquid chromatography mass spectrometry for PIP analysis. PIP extracts were separated on an XBridge C8 column (Waters, Milford, MA). Mobile phase A was methanol/water/70% ethylamine (50:50:0.13). Mobile phase B was 2-propanol/70% ethylamine (100:0.13). The gradient was 95%/5% (A/B) to 10%/90% (A/B) over 15 min, after which it was held for 1 min, before returning to 95%/5% (A/B) over 1 min, followed by holding for 10 min for reequilibration. The flow rate was 30 μ L/min at 25°C using an LTQ Orbitrap mass spectrometer (Thermo-Fisher Scientific, Waltham, MA). Ion spray voltage was set to -4.0 kV in negative ion mode. Phospholipids were measured by a full scan of parent ion (MS1) within charge/mass ratio (m/z) 380–1,500 in negative ion mode using an Orbitrap FTMS (Fourier transform mass spectrometry) analyzer with a resolution of 60,000. Mass accuracy was within 3 ppm. MS/MS (MS2) measurements at a collision energy setting of 35% were performed with an LTQ-IT (ion trap) analyzer when needed. PIP₁- and PIP₂-specific fragments (m/z 321 and 401, respectively) observed in MS2 were used for identification.

Cyclic phosphatidic acid/LPA/lysophosphatidylcholine assay. Cells were extracted with methanol:chloroform (2:1) containing 1 nmol/L ¹³C₁₆ LPA (18). The organic layer was dried under nitrogen and redissolved in 200 μ L of 0.1 mol/L ammonium acetate in methanol. Cyclic phosphatidic acid (CPA) and LPA were analyzed by LC-ESI-MS/MS (liquid chromatography coupled to tandem MS with electrospray ionization) using a modified protocol of Shan et al. (19). High-performance liquid chromatography separation was performed using an XBridge C18 column (50 \times 2.1 mm, 3 μ m; Waters). Mobile phase A consisted of 5 mmol/L ammonium acetate in water, adjusted to pH 9.9 with ammonium hydroxide. Mobile phase B was 60% acetonitrile and 40% isopropanol with a linear increase from 20% B to 99.5% B over 15 min, followed by a 5-min hold at 99.5% B. Online tandem MS analysis was performed using negative ion electrospray. Optimum multiple reaction monitoring (MRM) parameters were determined by flow-injection analysis of authentic standards and are listed in Supplementary Table 1. The parent ion for LPA and CPA species is the deprotonated molecular anion (M-H). Daughter ions for all LPA species were a common fragment at m/z 153.1. CPA species gave daughter ions, which were characterized by a common loss of 136. For lysophosphatidylcholine (LPC) analysis, samples were extracted by a mixture of methanol:chloroform and analyzed as previously described (20) using an Ascentis C18 column 15 cm \times 2.1 mmol/L \times 3 μ m (Supelco) and a TOF-MS (Agilent) operated in negative ion mode. LPC 16:0 was detected as a formic acid adduct with accurate mass of 540.3306 (<1 ppm error). Thin layer chromatography for PA and LPA analysis was performed as previously described (18).

Luciferase assay. NIH3T3 cells (5×10^6) were electroporated with vectors containing PPAR γ 1, AGPAT2, RXR α , and FATP-luciferase (1 μ g each) and 1 μ g of either empty vector, Agpat1, or Agpat2 expression plasmids. After plating, the cells were treated with the vehicle or rosiglitazone for 18 h. Luciferase activity was normalized to β -gal.

Statistics. Data are expressed as mean \pm one SEM. Statistical significance was determined using a noncorrected two-tailed Student *t* test, unpaired assuming equal variance or ANOVA, as appropriate. A *P* value of <0.05 was considered significant.

RESULTS

Intact myogenesis but impaired adipogenesis in MDMCs from CGL subjects. Expanded single-cell MDMC isolates from vastus lateralis muscle biopsies from

two control individuals were differentiated with either adipogenic (MDI) or myogenic (2% horse serum) media to determine their lineage potential (Supplementary Fig. 1). About 30% of the cultures showed bipotential differentiation,

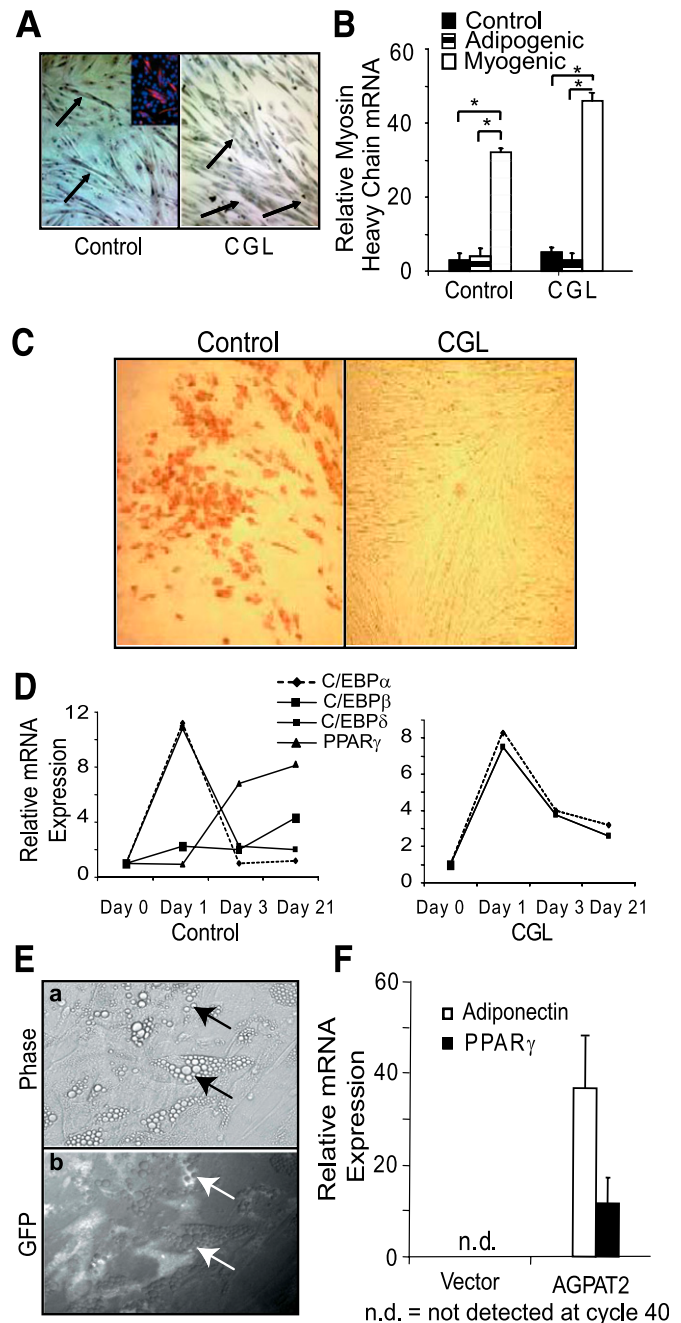


FIG. 1. Defective adipogenesis in CGL MDMCs. **A:** Formation of multi-nucleated cells in culture of CGL MDMCs (arrows). Cells were incubated in myocytic differentiation media (2% horse serum) for 10 days. Inset shows MF-20 staining. **B:** Expression of myosin heavy chain in CGL MDMCs after myocytic differentiation. *, *P* < 0.05. **C:** Oil Red O staining in adipogenic media ($\times 10$). **D:** mRNA profiles of control and CGL MDMCs after the addition of adipogenic media. Expression levels were normalized to 18s mRNA. C/EBP α and PPAR γ were not detected in CGL-derived MDMC cultures. Points represent an average of two experiments. **E:** Rescue of adipogenesis by expression of GFP-AGPAT2 in CGL MDMCs. **a:** Phase contrast image demonstrating the accumulation of lipid droplets (arrows). **b:** Cells showing GFP expression under fluorescent microscopy (original magnification $\times 40$). **F:** mRNA expression in CGL MDMCs after expression of GFP-AGPAT2. (A high-quality digital representation of this figure is available in the online issue.)

as evidenced by the formation of multinucleated cells staining for the myogenic marker Myf20 or the accumulation of lipid droplets positive for perilipin. Approximately 20% of the cells underwent adipogenesis only, 40–50% showed only myogenic differentiation, and a small percentage of the single-cell cultures could not be differentiated. Thus, individual human MDMCs undergo both myogenic and adipocytic differentiation.

MDMC cultures were obtained from two CGL subjects harboring defined AGPAT2 mutations (subjects 1 and 2) (Supplementary Table 2) (3). MDMC cultures from both control and CGL subjects were able to undergo myogenesis after exposure to 2% horse serum, demonstrated by the appearance of elongated, multinucleate cells (Fig. 1A) and increased expression of myosin heavy chain mRNA (Fig. 1B). In contrast to controls, CGL MDMC cultures exposed to MDI showed no accumulation of lipid droplets (Fig. 1C). C/EBP β and C/EBP δ mRNA rose in both control and CGL-derived culture (Fig. 1D) after 1 day of MDI treatment, and by 3 and 21 days, control culture showed induction of C/EBP α and PPAR γ whereas CGL cells showed no (threshold cycle > 40) PPAR γ or C/EBP α expression (Fig. 1D), indicating an ability to initiate adipogenesis while displaying a block in terminal differentiation.

The adipogenic defect in MDMCs from CGL patients was overcome by retroviral expression of GFP-tagged AGPAT2, as demonstrated by accumulation of lipid droplets in GFP-expressing cells (Fig. 1E) and increases in PPAR γ and adiponectin mRNA expression (Fig. 1F) after MDI exposure, consistent with the induction of the adipogenic program after AGPAT2 rescue. Unlike AGPAT2, infection of cells with GFP alone or GFP-tagged AGPAT1 did not result in the formation of lipid droplets (Supplementary Fig. 2).

AGPAT2, but not AGPAT1, regulates adipogenesis in 3T3-L1 cells. Due to the limited replicative life of MDMC cultures, we assessed the effect of manipulation of AGPAT2 in 3T3-L1 preadipocytes. Using a pool of siRNA for AGPAT1 or AGPAT2 or a nontargeting siRNA we were able to decrease mRNA expression and protein levels of AGPATs (Fig. 2A). Knockdown of AGPAT1 had almost no effect on accumulation of lipid in 3T3-L1 cells, whereas AGPAT2 knockdown significantly impaired adipogenesis, as assessed by Oil Red O staining (Fig. 2B) and decreased expression of C/EBP α , PPAR γ , and adiponectin mRNA levels (Fig. 2C). Consistent with a role in adipogenesis, AGPAT2 mRNA and protein levels increase markedly during differentiation of both 3T3-L1 cells and MDMCs (Supplementary Fig. 3). When 3T3-L1 preadipocytes were transfected with either V5-tagged AGPAT2 or empty vector,

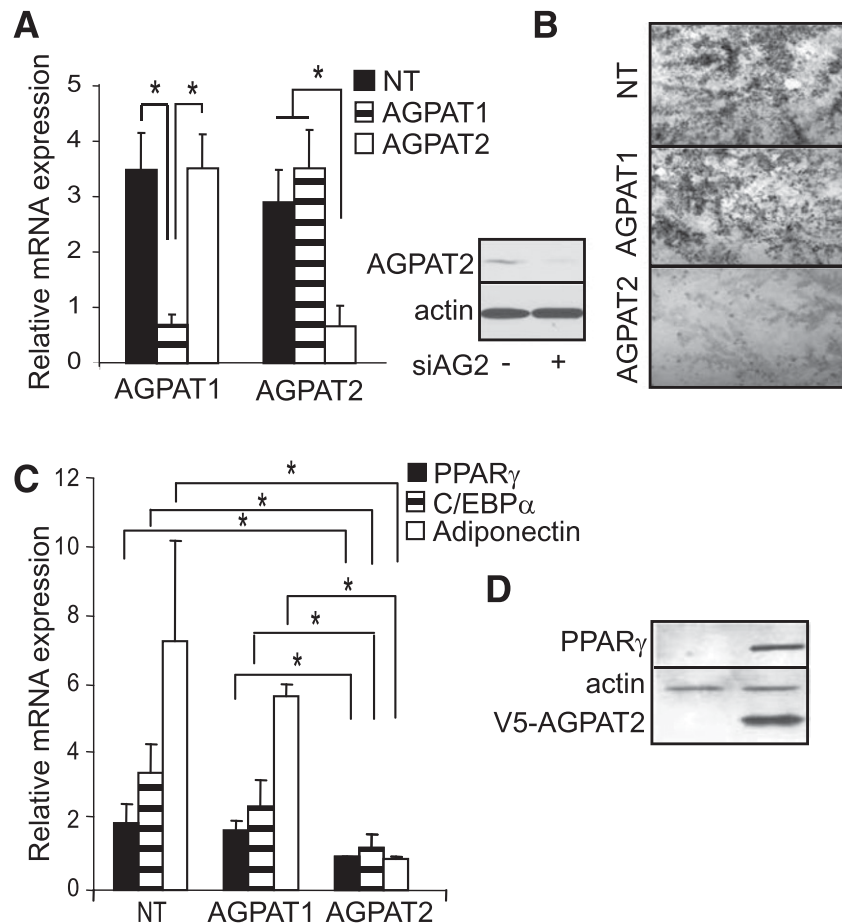


FIG. 2. AGPAT2 downregulation inhibits adipogenesis in 3T3-L1 cells. **A:** Changes in AGPAT mRNA levels in 3T3-L1 cells 48 h after treatment with nontargeting (NT), AGPAT1, or AGPAT2 siRNA. Expression levels were normalized to 18s mRNA levels \pm SD. * P < 0.05. **B:** Oil Red O staining of 3T3-L1 cells after 7 days of differentiation in adipogenic media after treatment with NT, AGPAT1, or AGPAT2 siRNA. Original magnification \times 10. **C:** Levels of adipogenesis-related genes after 4 days of differentiation after treatment with scrambled siRNA or AGPAT siRNA. Values are the mean of three independent determinations \pm SD. * P < 0.05. **D:** PPAR γ protein levels in 3T3-L1 cells expressing pc-DNA or V5-AGPAT2 after 48 h of insulin stimulation (300 nmol/L).

we found that overexpression of AGPAT2 increased protein levels of PPAR γ when compared with cells treated with an empty vector (Fig. 2D). Thus, modulation of AGPAT2 levels in 3T3-L1 preadipocytes parallels the phenotype of CGL-derived MDMCs.

Increased cell death after induction of adipogenesis in the absence of AGPAT2. We noted that during differentiation of MDMCs from CGL patients and in 3T3-L1 cells after AGPAT2 knockdown, there was an increase in cells lifting from the plates, suggesting cell death. AGPAT2, but not AGPAT1, knockdown resulted in a statistically significant reduction in the number of cells in the first 24 h of differentiation (Fig. 3A). This correlated with an increase in cell death, as demonstrated by propidium iodide staining (Fig. 3B). A similar effect was found in MDMCs from CGL patients assessed by flow cytometry. Prior to addition of the adipogenic media, no significant difference in annexin staining was seen between the control and CGL subjects (Fig. 3C). After 3 days of differentiation, the control MDMCs showed between 9.4 and 10.5% cell death, and the CGL cells from subjects 1 and 2 had 24 and 18.3%, respectively, annexin-positive cells (Fig. 3C), indicating significant cell compromise in the absence of AGPAT2.

AGPAT2 regulates the PI3K/Akt pathway. A key survival signal with a central role in adipogenesis is the PI3K/Akt pathway. Previous studies with small-molecule AGPAT2 inhibitors showed a reduction in Akt and Erk signaling in cancer cells (21–24). In adipocytes, insulin

stimulated Akt phosphorylation in MDMC cultures isolated from control individuals but was reduced in CGL-derived MDMC cultures, whereas Erk1/2 phosphorylation was preserved (Fig. 4A). Similarly, insulin-stimulated 3T3-L1 preadipocytes transfected with AGPAT2 siRNA showed significant attenuation of Akt phosphorylation as well as decreased phosphorylation of its downstream target p70-S6K1 (Fig. 4B). We corroborated our findings using two different siRNA sequences and both demonstrated a decrease in pSer473-Akt with good correlation between degree of AGPAT2 knockdown and downregulation of Akt phosphorylation (Supplementary Fig. 4). Unlike the Akt pathway, and consistent with the findings in human MDMCs, Erk1/2 phosphorylation was modestly upregulated in preadipocytes after AGPAT2 siRNA treatment (Fig. 4B).

To investigate gain of function by AGPAT2 overexpression, 3T3-L1 preadipocyte cells were transiently transfected with empty vector, V5-tagged AGPAT1, or V5-tagged AGPAT2. After 36 h, the cells were starved overnight and stimulated with insulin. AGPAT2 overexpression increased p473-Akt and p308-Akt phosphorylation, even in the absence of insulin stimulation, which correlated with an increase in the phosphorylation of p70-S6K1 (Fig. 4C). In contrast, AGPAT1 did not upregulate Akt phosphorylation but did increase the phosphorylation of p70-S6K1 (Fig. 4C). The efficacy of AGPAT2 to increase Akt phosphorylation appeared to be augmented by the addition of a mixture of free fatty acids, with increases in Akt phosphorylation in the presence of low insulin concentrations (50 nmol/L) and increased levels with higher concentrations (100 nmol/L) (Supplementary Fig. 5), suggesting an interactive role of AGPAT2 and fatty acids in enhancing preadipocyte signaling.

Consistent with its ability to increase Akt signaling, treatment of 3T3-L1 cells with insulin caused the nuclear exclusion of FoxO1 (Fig. 4D, a and b) (25). Cells overexpressing AGPAT2 demonstrated nuclear exclusion of FoxO1, even in the absence of insulin (Fig. 4D, c–e). Akt has been reported to migrate into the nucleus in response to a variety of proliferative stimuli, including insulin (26,27). Immunostaining 3T3-L1 cells for Akt in the presence or absence of insulin stimulation in control cells demonstrated the characteristic nuclear pattern of Akt (Supplementary Fig. 6A and B). Immunostaining of Akt in cells overexpressing GFP-AGPAT2 after starvation in serum-free media demonstrated translocation of Akt, even in the absence of insulin stimulation (Supplementary Figure 6C–E). Finally, we expressed constitutively active Akt (myr-Akt) after knockdown of AGPAT2 and then treated cells with MDI to induce differentiation. myr-Akt increased the expression of adiponectin, but not PPAR γ mRNA (Fig. 4E), and led to an increase in Oil Red O staining (Fig. 4F). These data demonstrate that disruption of AGPAT2 results in a significant reduction in Akt activation and downstream Akt signaling events, and bypassing this defect can rescue adipogenesis.

AGPAT2 regulates the phosphoinositide pathway. The generation of phosphatidylinositols is important for the activation of Akt signaling (28–32). Using LC/MS, we analyzed lipid extracts from 3T3-L1 preadipocytes expressing either GFP or AGPAT2-GFP. We found that overexpression of AGPAT2 results in a significant increase in both PIP₂ 36:1 and PIP₂ 36:2 levels without changes in PIP₁ levels (Fig. 5A). PIP₃ could not be assayed by LC/MS; however, immunofluorescence detected with anti-PIP₃

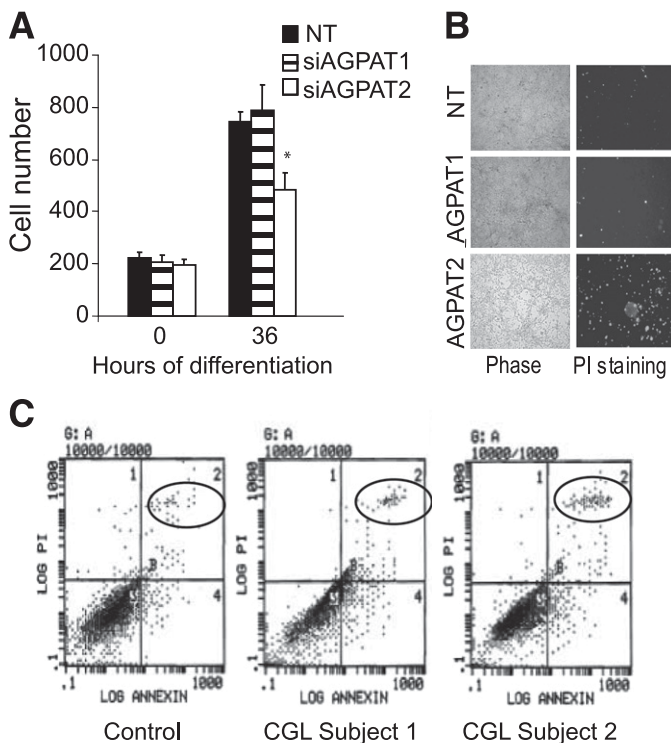


FIG. 3. AGPAT2 loss increases cell death in 3T3-L1 preadipocytes and CGL MDMCs. **A:** Quantification of cell number of 3T3-L1 cells treated with AGPAT2 siRNA at day 0 and 48 h after the addition of adipogenic media. $n = 3$. * $P < 0.01$. **B:** Propidium iodide (PI) staining of 3T3-L1 cells after siRNA treatment. Bright field (*left*). Cells under fluorescent microscopy (rhodamine filter) (*right*). **C:** Fluorescent cell sorting of control and CGL cells at baseline and 4 days after the addition of adipogenic media. Annexin fluorescence is the x-axis and propidium iodide fluorescence is the y-axis. Note increase in cell death in CGL cells at day 4.

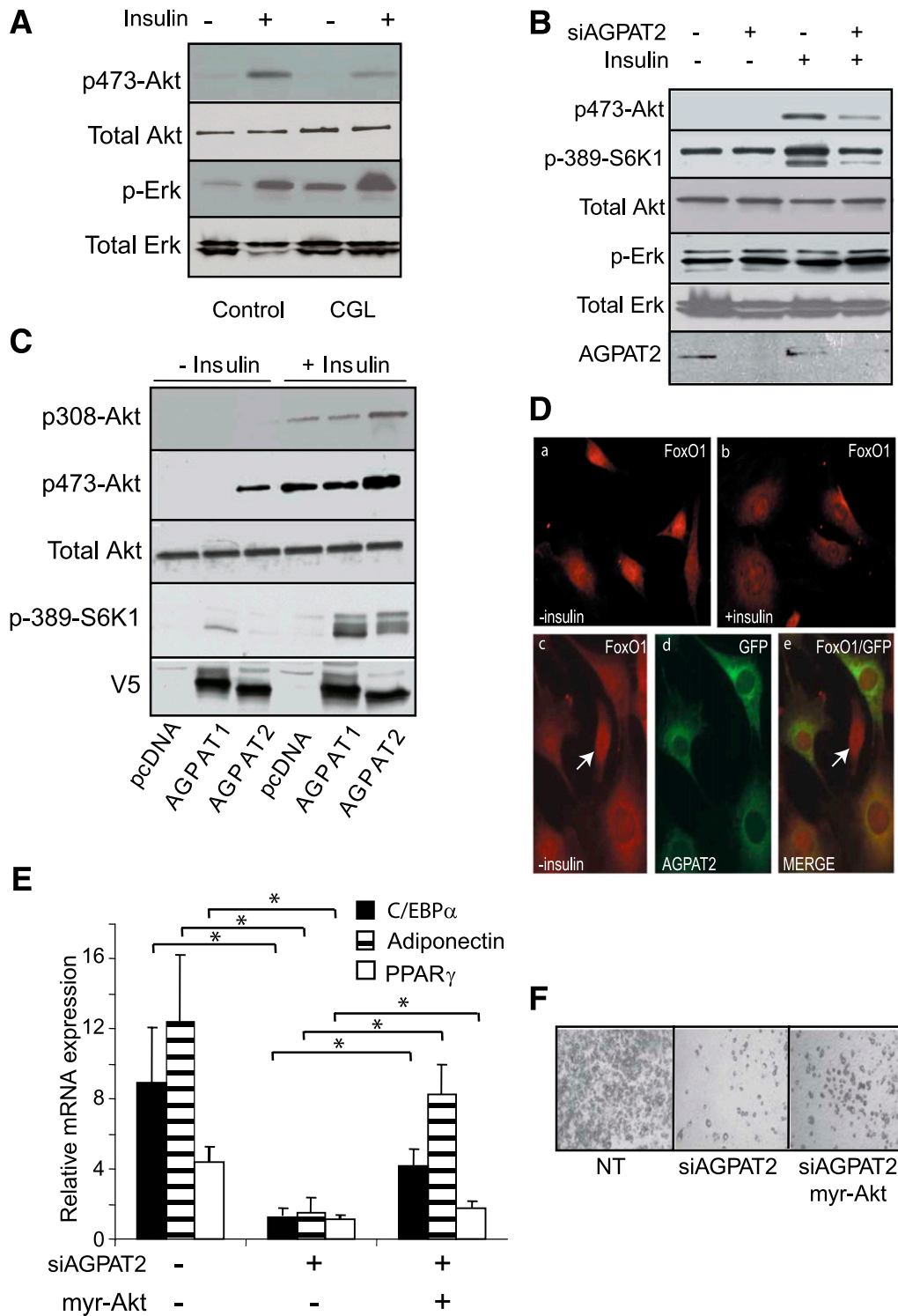


FIG. 4. Effect of AGPAT2 on insulin signaling events in 3T3-L1 cells and human MDMCs. **A:** MDMCs from control and CGL subjects were starved for 6 h in serum-free media and treated with insulin (50 nmol/L). Protein extracts were probed with the indicated antibodies. **B:** Effect of AGPAT2 siRNA on Akt and S6K1 phosphorylation after 6 h starvation for serum and treatment with insulin (50 nmol/L). **C:** Cells were transfected with either pc-DNA, V5-AGPAT1, or V5-AGPAT2 for 2 days. After 6 h starvation, cells were treated with 50 nmol/L insulin, and protein extracts were probed for the indicated antibodies. **D:** 3T3-L1 adipocytes were exposed to buffer (a) or 59 μmol/L insulin (b), fixed, and immunostained for FoxO1. Note the nuclear exclusion of FoxO1 after insulin stimulation. GFP-AGPAT2–transfected 3T3-L1 adipocytes were serum starved and immunostained for FoxO1 (c) or GFP visualized (d). Merged figure (e) shows reduced FoxO1 in GFP+ cells. Arrow depicts cell not expressing GFP-AGPAT2 with nuclear localization of FoxO1. **E:** 3T3-L1 cells treated with scrambled or AGPAT2 siRNA and transfected with myr-Akt where indicated. Cells were harvested after 4 days of differentiation, and mRNA levels were quantified. *n* = 4 for each condition; mean ± SD. **P* < 0.05. **F:** Oil Red O staining of 3T3-L1 cells after 7 days of differentiation in adipogenic media after treatment with scrambled siRNA (nontargeting [NT]), AGPAT2 siRNA, or AGPAT2 siRNA with myr-Akt. Original magnification ×20. (A high-quality digital representation of this figure is available in the online issue.)

antibody was increased after AGPAT2 overexpression and was confirmed by quantification using direct detection on nitrocellulose membranes (Fig. 5B and C). Consistent with a role for AGPAT2 regulating the upstream signaling to Akt, we found that in serum-starved 3T3-L1 preadipocytes, AGPAT2 overexpression resulted in increased Akt phosphorylation, which was completely abrogated by the PI3K inhibitor LY294002 (Fig. 5D). The findings support a role for AGPAT2 as regulator of phosphatidylinositol levels in preadipocytes, which in turn modulates Akt signaling.

Effect of AGPAT1 and AGPAT2 on PPAR γ activity and glycerolipid levels. LPA has been described as an endogenous PPAR γ agonist, whereas CPA was recently identified as a PPAR γ antagonist with nanomolar affinity (33,34). CPA is a naturally occurring analog of LPA, and although both share a similar structure, their biological effects differ significantly (35). We assessed the effect of AGPAT1 and AGPAT2 on PPAR γ transactivation and endogenous levels of these bioactive lipids. When NIH3T3 cells were transfected with AGPAT1 or AGPAT2, only AGPAT2 increased expression of a PPAR γ luciferase promoter driven by a canonical PPAR-responsive element

(PPRE) (36), both in the absence and presence of the PPAR γ ligand rosiglitazone (Fig. 6A). This was not associated with a significant increase in PPAR γ protein levels or migration, suggesting that AGPAT2 overexpression modulates the transactivation of PPAR γ (Fig. 6B). It was possible that the effect of AGPAT2 overexpression on PPAR γ activity was dependent on the activation of the PI3K/Akt pathway. Cells treated with the PI3K inhibitor LY294002 demonstrated ~50% downregulation of luciferase activity (Fig. 6B). However, AGPAT2 overexpression increased the luciferase expression in both control and LY294002-treated cells, suggesting that the effect of AGPAT2 was independent of the direct activation of Akt.

Knockdown of AGPAT2 resulted in an increase in different LPA species (Fig. 7A), and, surprisingly, overexpression of AGPAT1 and AGPAT2 also resulted in an increase in the levels of LPA (Fig. 7B) while simultaneously decreasing PA. Conversely, knockdown of AGPAT2 resulted in increased levels of the PPAR γ inhibitor CPA, in particular

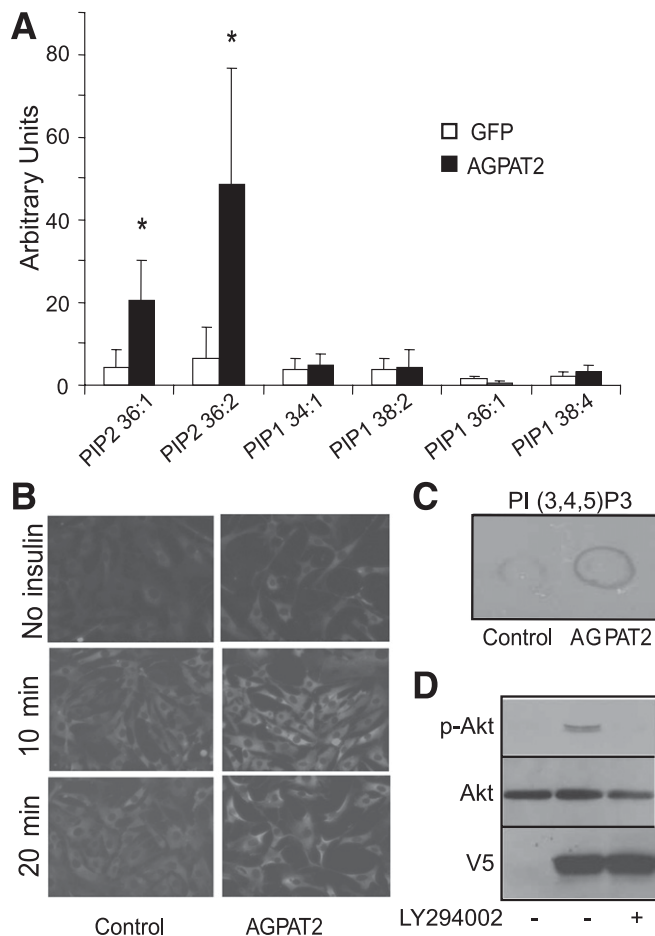


FIG. 5. AGPAT2 increases PIP₂ and PIP₃. **A:** 3T3-L1 cells expressing GFP or GFP-AGPAT2 were harvested under basal conditions. Lipid extracts were analyzed with LC/MS. $n = 5$ for each condition; mean \pm SD. $*P < 0.05$. **B:** Immunostaining for PIP₃ of cells after 6 h starvation and insulin stimulation for the indicated times. **C:** PIP₃ blot from lipid extracts of the same cells in serum-replete media. **D:** 3T3-L1 cells transfected with either empty vector or AGPAT2 were starved for 6 h in serum-free media and treated with LY294002 10 nmol/L for 20 h, where indicated. Protein extracts were probed for the indicated antibodies.

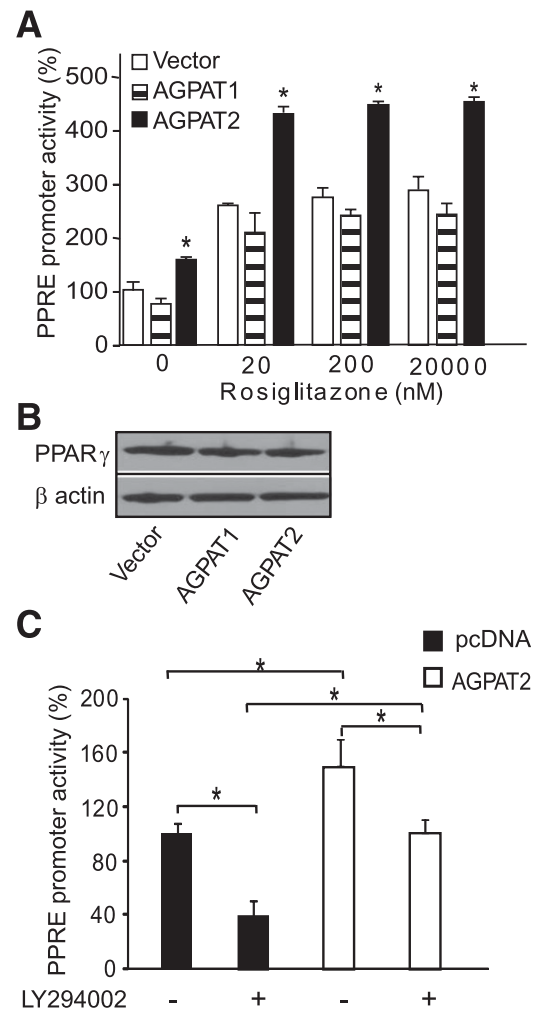


FIG. 6. AGPAT2 increases PPAR γ transactivation independent of PI3K. **A:** NIH3T3 cells were transfected with empty vector, AGPAT1, or AGPAT2 and PPREx3-LUC reporter, RXR α , and PPAR γ . Cells were treated with rosiglitazone for 20 h, and relative luciferase activity was quantified. $n = 4$ for each condition; mean \pm SD. $*P < 0.05$. **B:** PPAR γ protein levels at 48 h of transfection. β -Actin was used as loading control. **C:** NIH3T3 cells were transfected with empty vector or AGPAT2 and PPREx3-LUC reporter, RXR α , and PPAR γ . Cells were treated with LY294002 (10 nmol/L) for 20 h, and relative luciferase activity was quantified. $n = 3$ for each condition; mean \pm SD. $*P < 0.05$.

the most highly abundant subspecies, CPA18:0 and CPA16:0 (Fig. 7C). Overexpression of AGPAT2 decreased CPA levels of the same subspecies, whereas overexpression of AGPAT1 had no effect or a trend toward increasing CPA species (Fig. 7D). LPC, the precursor of CPA, has been implicated as a negative regulator of insulin signaling and is also reduced (~20%) after overexpression of AGPAT2 (Supplementary Fig. 7) (37). The ability of pioglitazone and

AGPAT2 to enhance transactivation of the PPAR γ reporter was inhibited by treatment with exogenous CPA, suggesting that AGPAT2 modulates the production of CPA rather than increasing its turnover (Fig. 7E). Finally, to determine the role of PPAR γ transactivation on the adipogenic defect of CGL-derived MDMCs, we treated cells derived from subject 2 with the PPAR γ agonist pioglitazone along with MDI. Pioglitazone increased the expression of

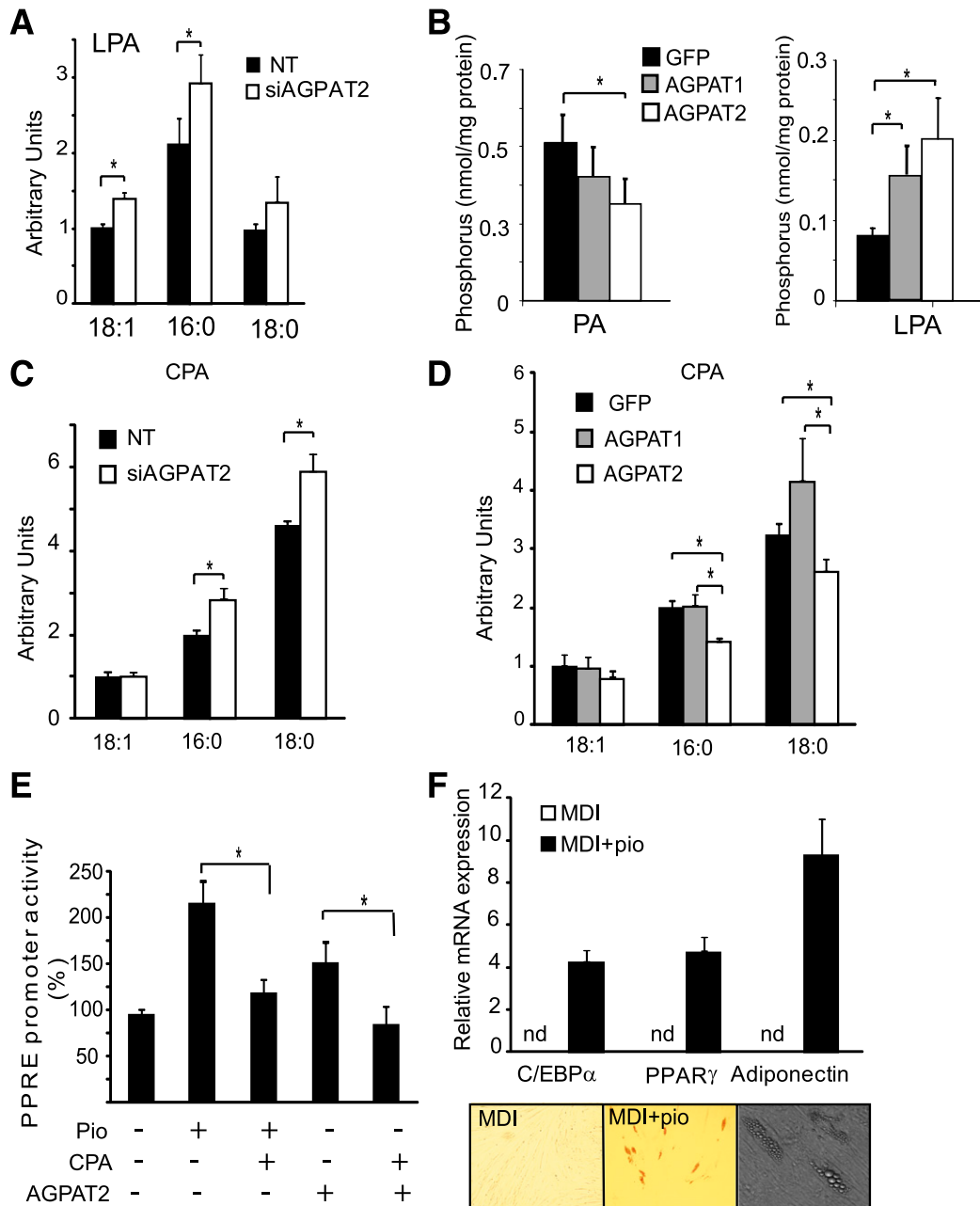


FIG. 7. Effect of AGPAT2 on glycerophospholipids. **A:** 3T3-L1 cells were treated with siRNA either nontargeting (NT) or AGPAT2, and LPA levels were determined through LC/MS after 3 days. $n = 4$ for each condition; mean \pm SD. $*P < 0.05$. **B:** 3T3-L1 cells overexpressing AGPAT2 or empty vector underwent lipid extraction and subsequent thin-layer chromatography separation. Phosphatidic acid and LPA levels were determined. $n = 4$ for each condition; mean \pm SD. $*P < 0.05$. **C:** 3T3-L1 cells treated with scrambled or AGPAT2 siRNA were harvested and phospholipids were extracted for LC/MS analysis. CPA levels were determined after 3 days. $n = 4$ for each condition; mean \pm SD. $*P < 0.05$. **D:** Quantification of CPA by LC/MS levels in 3T3-L1 cells overexpressing GFP or AGPAT2. $n = 4$ for each condition; mean \pm SD. $*P < 0.05$. **E:** NIH3T3 cells were transfected with empty vector or AGPAT2 and PPREx3-LUC reporter, RXR α , and PPAR γ . Cells were treated with pioglitazone or CPA, where indicated, for 20 h, and relative luciferase activity was quantified. $n = 4$ for each condition; mean \pm SD. $*P < 0.05$. **F:** mRNA profiles and representative Oil Red O staining of CGL MDMCs after the addition of MDI media with or without pioglitazone (10 nmol/L) after 12 days of differentiation. $n = 4$ for each condition; mean \pm SD. nd, not determined. (A high-quality color representation of this figure is available in the online issue.)

terminal differentiation markers *C/EBP α* and *PPAR γ* , and this associated with the accumulation of lipid droplets, as shown by Oil Red O staining (Fig. 7*F*), though this effect was still significantly reduced compared with the differentiation observed in cells from control individuals.

DISCUSSION

AGPAT2 mutations have been found in a subset of patients with CGL, and it was presumed that these subjects were unable to generate triglycerides, resulting in “empty adipocytes” (3). However, earlier studies suggested that AGPAT2 is involved in adipogenesis. Our work in MDSCs from humans with AGPAT2 mutations as well as in 3T3-L1 cells shows that AGPAT2 plays a central role in adipogenesis by generating a proadipogenic lipome, leading to the activation of Akt signaling while

simultaneously regulating the production of CPA, a *PPAR γ* inhibitor.

AGPAT2 is upregulated in a number of tumors, including ovarian cancer (38,39) and small-molecule inhibitors have been developed that specifically inhibit AGPAT2. These agents result in the attenuation of a number of signaling pathways, including both the Ras/Raf/Erk and PI3K/Akt pathways (9). Our work demonstrates that gain and loss of AGPAT2, but not AGPAT1, has concordant effects on the phosphorylation of Akt and its downstream targets. Further, we find that constitutively active Akt can partially rescue the adipogenic defect, demonstrating that loss of AGPAT2 is working proximal to Akt activation. In the absence of AGPAT2, differentiating CGL-derived progenitor cells had increased cell death, similar to AGPAT2-expressing tumor cells after treatment with an AGPAT2-specific small-molecule inhibitor, suggesting that apoptosis of differentiating

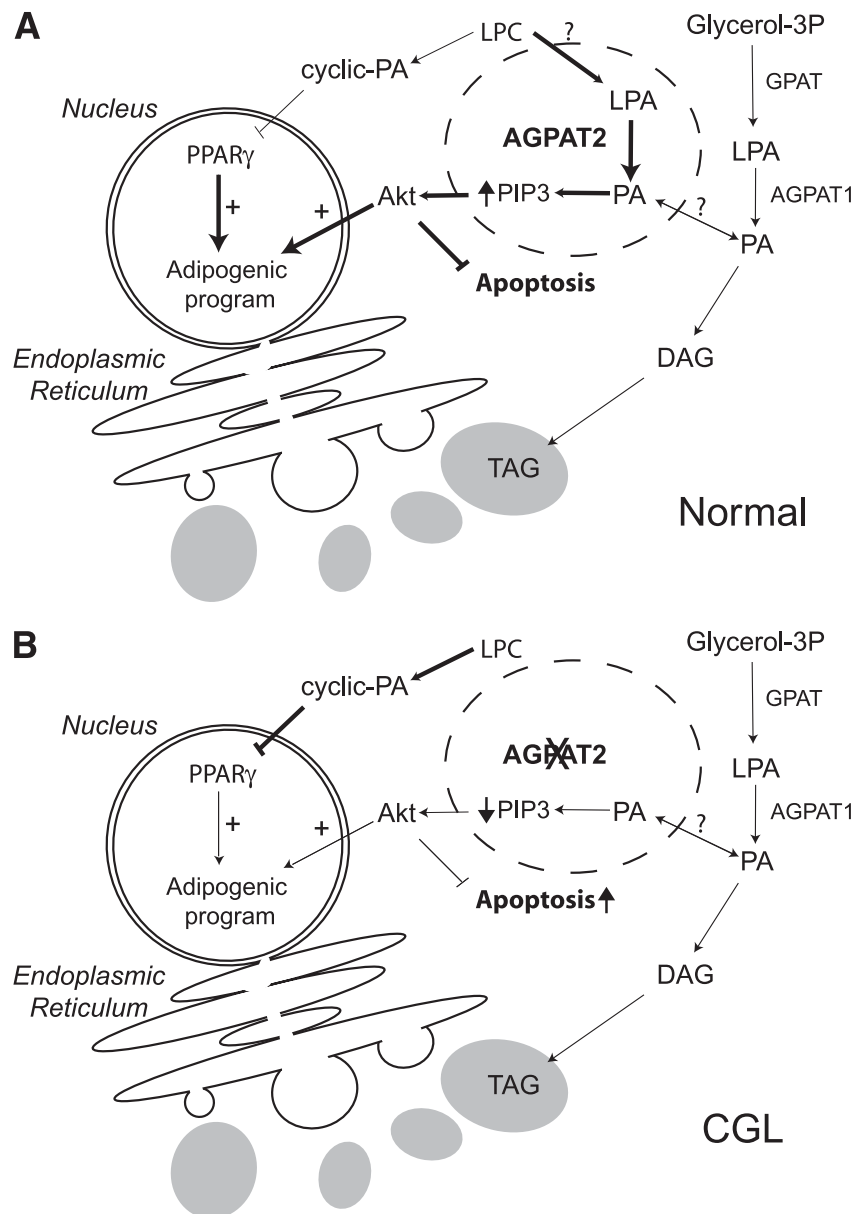


FIG. 8. Schematic representation of AGPAT2 regulation of adipogenesis. Schematic of proposed role of AGPAT2 in supporting adipocyte differentiation from normal individuals (A) and changes in people with CGL (B). See text for details.

adipocytes may play a role in the severe lipodystrophic phenotype seen in CGL patients. Both Akt and PPAR γ are involved in adipocyte survival (40). A provocative observation is that addition of fatty acids to cells overexpressing AGPAT2 further increases Akt phosphorylation, suggesting a physiological mechanism whereby increased flux of fatty acids may participate in the stimulation of the adipogenic program. Further work on the specificity of fatty acids and concentration and duration of exposure will be important to define these relationships.

We continue to try to understand the apparently paradoxical effects of AGPAT2 on PA and LPA levels in cells. Ovarian cancer cells in which AGPAT2 is highly expressed show an increase in LPA levels, and knockdown of AGPAT2 in OP9 cells results in increases in PA levels, identical to our findings (41). As with AGPAT2, disruption of the *Lipin-1* gene results in lipodystrophy in mice (42, 43). PA results in Lipin-1 exclusion from the nucleus and accumulation in the endoplasmic reticulum (44,45). One potential explanation for the paradoxical PA changes is that the PA pool affected by AGPAT2 is not reflected in total cells extracts. In preliminary studies, we have found that AGPAT2 overexpression causes the nuclear exclusion of Lipin-1 (A.R.S., unpublished observation), which is consistent with a localized increase of PA in the endoplasmic reticulum. Further studies will be needed to sort out the complex changes in lipid metabolism that result in unexpected changes in bulk PA and LPA levels in cells after alterations in AGPAT2 expression.

Although AGPAT2 mRNA is detected in 3T3-L1 preadipocytes prior to differentiation, there is a significant increase after induction of adipogenesis, paralleling that of PPAR γ , and it is also increased in vivo after treatment with the PPAR γ agonist pioglitazone (46), placing AGPAT2 as a PPAR γ -responsive gene. Sequence analysis shows a PPAR direct repeat at -723 from the transcriptional start site. The finding that AGPAT2 reduces CPA levels in preadipocytes could suggest that the progressive increase in PPAR γ with differentiation is accompanied by reduction in CPA levels, allowing activation of PPAR γ . These findings support a model in which AGPAT2 joins PPAR γ and c/EBP α as part of a positive feedback loop promoting the mature adipocyte phenotype.

Treatment of CGL-derived MDMCs with pioglitazone was able to increase the expression of adipocyte terminal differentiation markers and generate lipid droplets, although this effect was markedly attenuated compared with MDMCs derived from control individuals. Despite the almost complete absence of adipose tissue, subject 3 (Supplementary Table 2) responded to therapy with PPAR γ agonists. Her HbA_{1c} was reduced from 14.6 to 9.7% and her triglycerides decreased from 727 mg/dL to 213 mg/dL after 6 months of treatment (47). Considering the in vitro response of MDMCs to pioglitazone, it is tempting to suggest that generation of adipocytes from precursor cells helped alleviate some of the metabolic derangements in this patient, although it is possible that thiazolidinedione exerted its metabolic effect independent of adipose tissue (48–50). AGPAT2 and PPAR γ are both expressed in other insulin-responsive tissues, including liver and skeletal muscle. This would raise the possibility that AGPAT2 is important for the regulation of PPAR γ and PI3K/Akt in tissues, which contributes to the severe insulin resistance in CGL patients. Although AGPAT2 is expressed in liver, the hepatic steatosis seen in CGL subjects appears to be secondary to the insulin

resistance and not to a direct effect of AGPAT2 on hepatic lipogenesis (51).

In summary, this study provides a further understanding of the pathogenesis of lipodystrophy in patients with AGPAT2 mutations. Our findings demonstrate that CGL secondary to AGPAT2 mutation is not a disease of empty adipocytes, rather a disease of defective adipose tissue development due to a disruption in the modulation of the lipome during adipogenesis (Fig. 8). Normally, upon activation of the differentiation program, AGPAT2 expression increases and reduces cyclic PA levels, possibly by directing LPA generated from LPC to PA. This allows endogenously derived PPAR γ activators to increase PPAR γ -mediated activation of the adipogenic program. The increased flux to PA could be the basis for increasing the generation of PIP₃, which is important for activation of Akt. Because of the paradoxical change in LPA in cells with AGPAT2 manipulation, we believe that the PA generated by AGPAT2 is compartmentalized from that generated by AGPAT1 (Fig. 8A, dashed circle). In patients with CGL due to AGPAT2 mutations, cyclic PA increases and inhibits PPAR γ , and the reduced generation of PA could be leading to reduced PIP₃ levels, impaired activation of Akt, and an increase in apoptosis (Fig. 8B). Understanding AGPAT2 actions in adipogenesis in relation to the modulation of the lipome provides the potential for understanding the intimate relationship between lipids, adipogenesis, lipid metabolism, and insulin resistance in common obesity.

ACKNOWLEDGMENTS

This work was supported by the Michigan Nutrition Obesity Research Center (DK-089503) Metabolomics Core and Pilot Grant Program and by the Robert C. and Veronica Atkins Research Foundation.

No potential conflicts of interest relevant to this article were reported.

A.R.S. designed and performed the experiments and wrote the manuscript. A.K.D., X.L., B.E., C.E., M.E.A., and M.T. performed the experiments. E.O. and T.L. contributed to the experiments and manuscript preparation. C.F.B. contributed to experimental design and writing and editing the manuscript. C.F.B. and A.R.S. are the guarantors of this work and, as such, had full access to all the data in the study and take responsibility for the integrity of the data and the accuracy of the data analysis.

REFERENCES

- Huang-Doran I, Sleight A, Rochford JJ, O'Rahilly S, Savage DB. Lipodystrophy: metabolic insights from a rare disorder. *J Endocrinol* 2010;207:245–255
- Cao H, Alston L, Ruschman J, Hegele RA. Heterozygous CAV1 frameshift mutations (MIM 601047) in patients with atypical partial lipodystrophy and hypertriglyceridemia. *Lipids Health Dis* 2008;7:3
- Agarwal AK, Arioglu E, De Almeida S, et al. AGPAT2 is mutated in congenital generalized lipodystrophy linked to chromosome 9q34. *Nat Genet* 2002;31:21–23
- Miranda DM, Wajchenberg BL, Calsolari MR, et al. Novel mutations of the BSCL2 and AGPAT2 genes in 10 families with Berardinelli-Seip congenital generalized lipodystrophy syndrome. *Clin Endocrinol (Oxf)* 2009;71:512–517
- Leung DW. The structure and functions of human lysophosphatidic acid acyltransferases. *Front Biosci* 2001;6:D944–D953
- Simha V, Garg A. Phenotypic heterogeneity in body fat distribution in patients with congenital generalized lipodystrophy caused by

- mutations in the AGPAT2 or seipin genes. *J Clin Endocrinol Metab* 2003; 88:5433–5437
7. Bonham L, Leung DW, White T, et al. Lysophosphatidic acid acyltransferase-beta: a novel target for induction of tumour cell apoptosis. *Expert Opin Ther Targets* 2003;7:643–661
 8. Hideshima T, Chauhan D, Hayashi T, et al. Antitumor activity of lysophosphatidic acid acyltransferase-beta inhibitors, a novel class of agents, in multiple myeloma. *Cancer Res* 2003;63:8428–8436
 9. Coon M, Ball A, Pound J, et al. Inhibition of lysophosphatidic acid acyltransferase beta disrupts proliferative and survival signals in normal cells and induces apoptosis of tumor cells. *Mol Cancer Ther* 2003;2:1067–1078
 10. Gale SE, Frolov A, Han X, et al. A regulatory role for 1-acylglycerol-3-phosphate-O-acyltransferase 2 in adipocyte differentiation. *J Biol Chem* 2006;281:11082–11089
 11. Wada MR, Inagawa-Ogashiwa M, Shimizu S, Yasumoto S, Hashimoto N. Generation of different fates from multipotent muscle stem cells. *Development* 2002;129:2987–2995
 12. Williams JT, Southerland SS, Souza J, Calcutt AF, Cartledge RG. Cells isolated from adult human skeletal muscle capable of differentiating into multiple mesodermal phenotypes. *Am Surg* 1999;65:22–26
 13. Asakura A, Komaki M, Rudnicki M. Muscle satellite cells are multipotential stem cells that exhibit myogenic, osteogenic, and adipogenic differentiation. *Differentiation* 2001;68:245–253
 14. Cossu G, De Angelis L, Borello U, et al. Determination, diversification and multipotency of mammalian myogenic cells. *Int J Dev Biol* 2000;44:699–706
 15. Subauste AR, Burant CF. Role of FoxO1 in FFA-induced oxidative stress in adipocytes. *Am J Physiol Endocrinol Metab* 2007;293:E159–E164
 16. Ogiso H, Taguchi R. Reversed-phase LC/MS method for polyphosphoinositide analyses: changes in molecular species levels during epidermal growth factor activation in A431 cells. *Anal Chem* 2008;80:9226–9232
 17. Bligh EG, Dyer WJ. A rapid method of total lipid extraction and purification. *Can J Biochem Physiol* 1959;37:911–917
 18. Subauste AR, Elliott B, Das AK, Burant CF. A role for 1-acylglycerol-3-phosphate-O-acyltransferase-1 in myoblast differentiation. *Differentiation* 2010;80:140–146
 19. Shan L, Li S, Jaffe K, Davis L. Quantitative determination of cyclic phosphatidic acid in human serum by LC/ESI/MS/MS. *J Chromatogr B Analyt Technol Biomed Life Sci* 2008;862:161–167
 20. Sato Y, Nakamura T, Aoshima K, Oda Y. Quantitative and wide-ranging profiling of phospholipids in human plasma by two-dimensional liquid chromatography/mass spectrometry. *Anal Chem* 2010;82:9858–9864
 21. Zhang HH, Huang J, Düvel K, et al. Insulin stimulates adipogenesis through the Akt-TSC2-mTORC1 pathway. *PLoS ONE* 2009;4:e6189
 22. Garg A, Agarwal AK. Lipodystrophies: disorders of adipose tissue biology. *Biochim Biophys Acta* 2009;1791:507–513
 23. Baudry A, Yang ZZ, Hemmings BA. PKBalpha is required for adipose differentiation of mouse embryonic fibroblasts. *J Cell Sci* 2006;119:889–897
 24. Longo KA, Kennell JA, Ochocinska MJ, Ross SE, Wright WS, MacDougald OA. Wnt signaling protects 3T3-L1 preadipocytes from apoptosis through induction of insulin-like growth factors. *J Biol Chem* 2002;277:38239–38244
 25. Nakae J, Kitamura T, Kitamura Y, Biggs WH 3rd, Arden KC, Accili D. The forkhead transcription factor Foxo1 regulates adipocyte differentiation. *Dev Cell* 2003;4:119–129
 26. Meier R, Alessi DR, Cron P, Andjelković M, Hemmings BA. Mitogenic activation, phosphorylation, and nuclear translocation of protein kinase Bbeta. *J Biol Chem* 1997;272:30491–30497
 27. Meier R, Hemmings BA. Regulation of protein kinase B. *J Recept Signal Transduct Res* 1999;19:121–128
 28. Magun R, Burgering BM, Coffey PJ, et al. Expression of a constitutively activated form of protein kinase B (c-Akt) in 3T3-L1 preadipose cells causes spontaneous differentiation. *Endocrinology* 1996;137:3590–3593
 29. Sakaue H, Ogawa W, Matsumoto M, et al. Posttranscriptional control of adipocyte differentiation through activation of phosphoinositide 3-kinase. *J Biol Chem* 1998;273:28945–28952
 30. Xia X, Serrero G. Inhibition of adipose differentiation by phosphatidylinositol 3-kinase inhibitors. *J Cell Physiol* 1999;178:9–16
 31. Kohn AD, Summers SA, Birnbaum MJ, Roth RA. Expression of a constitutively active Akt Ser/Thr kinase in 3T3-L1 adipocytes stimulates glucose uptake and glucose transporter 4 translocation. *J Biol Chem* 1996;271:31372–31378
 32. Sopasakis VR, Liu P, Suzuki R, et al. Specific roles of the p110alpha isoform of phosphatidylinositol 3-kinase in hepatic insulin signaling and metabolic regulation. *Cell Metab* 2010;11:220–230
 33. McIntyre TM, Pontsler AV, Silva AR, et al. Identification of an intracellular receptor for lysophosphatidic acid (LPA): LPA is a transcellular PPAR-gamma agonist. *Proc Natl Acad Sci USA* 2003;100:131–136
 34. Tsukahara T, Tsukahara R, Fujiwara Y, et al. Phospholipase D2-dependent inhibition of the nuclear hormone receptor PPARgamma by cyclic phosphatidic acid. *Mol Cell* 2010;39:421–432
 35. Tania M, Khan MA, Zhang H, Li J, Song Y. Autotaxin: a protein with two faces. *Biochem Biophys Res Commun* 2010;401:493–497
 36. Hegele RA, Cao H, Frankowski C, Mathews ST, Leff T. PPARG F388L, a transactivation-deficient mutant, in familial partial lipodystrophy. *Diabetes* 2002;51:3586–3590
 37. Han MS, Lim YM, Quan W, et al. Lysophosphatidylcholine as an effector of fatty acid-induced insulin resistance. *J Lipid Res* 2011;52:1234–1246
 38. Burton A. LPAAT-beta identifies aggressive ovarian cancer. *Lancet Oncol* 2006;7:893
 39. Springett GM, Bonham L, Hummer A, et al. Lysophosphatidic acid acyltransferase-beta is a prognostic marker and therapeutic target in gynecologic malignancies. *Cancer Res* 2005;65:9415–9425
 40. Imai T, Takakuwa R, Marchand S, et al. Peroxisome proliferator-activated receptor gamma is required in mature white and brown adipocytes for their survival in the mouse. *Proc Natl Acad Sci USA* 2004;101:4543–4547
 41. Pua TL, Wang FQ, Fishman DA. Roles of LPA in ovarian cancer development and progression. *Future Oncol* 2009;5:1659–1673
 42. Péterfy M, Phan J, Xu P, Reue K. Lipodystrophy in the fld mouse results from mutation of a new gene encoding a nuclear protein, lipin. *Nat Genet* 2001;27:121–124
 43. Zhang P, Takeuchi K, Csaki LS, Reue K. Lipin-1 phosphatidic acid phosphatase activity modulates phosphatidic acid levels to promote induction of peroxisome proliferator-activated receptor gamma (PPARgamma) gene expression during adipogenesis. *J Biol Chem* 2012;287:3485–3494
 44. Ren H, Federico L, Huang H, et al. A phosphatidic acid binding/nuclear localization motif determines lipin1 function in lipid metabolism and adipogenesis. *Mol Biol Cell* 2010;21:3171–3181
 45. Antonescu CN, Danuser G, Schmid SL. Phosphatidic acid plays a regulatory role in clathrin-mediated endocytosis. *Mol Biol Cell* 2010;21:2944–2952
 46. Yao-Borengasser A, Rassouli N, Varma V, et al. Stearoyl-coenzyme A desaturase 1 gene expression increases after pioglitazone treatment and is associated with peroxisomal proliferator-activated receptor-gamma responsiveness. *J Clin Endocrinol Metab* 2008;93:4431–4439
 47. Arioglu E, Duncan-Morin J, Sebring N, et al. Efficacy and safety of troglitazone in the treatment of lipodystrophy syndromes. *Ann Intern Med* 2000;133:263–274
 48. Burant CF, Sreenan S, Hirano K, et al. Troglitazone action is independent of adipose tissue. *J Clin Invest* 1997;100:2900–2908
 49. Norris AW, Chen L, Fisher SJ, et al. Muscle-specific PPARgamma-deficient mice develop increased adiposity and insulin resistance but respond to thiazolidinediones. *J Clin Invest* 2003;112:608–618
 50. Hevener AL, He W, Barak Y, et al. Muscle-specific Pparg deletion causes insulin resistance. *Nat Med* 2003;9:1491–1497
 51. Agarwal AK, Sukumaran S, Cortés VA, et al. Human 1-acylglycerol-3-phosphate O-acyltransferase isoforms 1 and 2: biochemical characterization and inability to rescue hepatic steatosis in *Apat2(-/-)* gene lipodystrophic mice. *J Biol Chem* 2011;286:37676–37691